

## Phase study of solid CO<sub>2</sub> to 20 GPa by infrared-absorption spectroscopy

K. Aoki, H. Yamawaki, and M. Sakashita

*National Institute of Materials and Chemical Research, Tsukuba, Ibaraki 305, Japan*

(Received 23 April 1993; revised manuscript received 10 June 1993)

A discrete change in the vibron frequency was observed in association with the transition from the cubic *Pa3* structure at about 12 GPa and ambient temperature. The pressure dependence of the vibron frequencies measured for the high-pressure phase up to 20 GPa was not in agreement with those calculated previously for a presumed high-pressure phase of an orthorhombic *Cmca* structure. Two Raman-active libron peaks observed in the high-pressure phase indicated that the primitive cell probably contained two molecules, instead of four as in the *Cmca* structure. These aspects of the vibron and libron spectra suggested that a tetragonal structure isomorphous with  $\gamma$ -N<sub>2</sub> was a more likely structure as the high-pressure phase of solid CO<sub>2</sub>.

### INTRODUCTION

CO<sub>2</sub> is a linear molecule with a large electric quadrupole moment. As a result of its strong mutual interactions, the molecules are arranged in a face-centered cubic lattice belonging to the *Pa3* space group,<sup>1</sup> in which the molecules are oriented along the body diagonal directions. The cubic *Pa3* structure thus stabilized exists over a wide pressure range.<sup>2,3</sup>

A new crystalline phase of CO<sub>2</sub> was observed under high pressure with a Raman-spectroscopy measurement.<sup>4</sup> New libron peaks appeared above 18 GPa at ambient temperature, indicating transition from the *Pa3* structure. This transition was immediately confirmed by the low-temperature Raman measurement.<sup>5</sup> At temperatures below 80 K the transition occurred at relatively low pressures around 11 GPa with a large hysteresis of the transition pressure.

Crystal structures and vibrational properties in solid CO<sub>2</sub> under pressure have intensively been studied using model potentials.<sup>6-9</sup> The latest free-energy calculations<sup>8,9</sup> showed that an orthorhombic *Cmca* structure isomorphous with solid CS<sub>2</sub> was the most favorable as the high-pressure phase. The calculated transition pressure, however, was significantly lower than the experimental results: 4.3 GPa at zero temperature and 11 GPa at 300 K. Moreover, the libron frequencies calculated for the predicted *Cmca* structure were not in agreement with those observed for the high-pressure phase. This was contrast to the excellent agreement in the same frequency calculation for the low-pressure *Pa3* phase. Hence, detailed measurements on the vibrational properties of the high-pressure phase and exact determination of the transition pressure are required to clarify further the phase transition in solid CO<sub>2</sub>.

In this paper, we report infrared data on solid CO<sub>2</sub> measured to 20 GPa and discuss aspects of the vibrational property of the high-pressure phase in relation to its crystal structure.

### HIGH-PRESSURE EXPERIMENT

Infrared spectra of solid CO<sub>2</sub> were measured with a gasketed diamond cell at various pressures and ambient

temperature. The cell was loaded with gaseous CO<sub>2</sub> of 99.995% purity at a temperature below the solidification temperature of 195 K and was warmed to room temperature for infrared measurement. Spectra were taken with a microscope Fourier transform infrared (FTIR) spectrometer with 1 cm<sup>-1</sup> resolution. The measuring area masked was 100×100 μm<sup>2</sup> and the pressure was determined from the peak shift of ruby fluorescence peak. Since pressure gradient was large in the sample chamber approximately 200 μm in diameter and 40 μm in thickness, two ruby chips occasionally located on both sides of the measuring area were chosen for pressure determination. The pressure difference at the two ruby chips was about 6% of their averaged pressure in the loading process and about 10% somewhat larger in the unloading process. Raman spectra were also measured in the libron frequency region in order to detect the phase transition distinctly.

### RESULTS

The CO<sub>2</sub> molecule has three normal vibrational modes, the symmetric stretching mode  $\nu_1$ , the bending mode  $\nu_2$ , and the antisymmetric mode  $\nu_3$ . Among them the  $\nu_2$  and

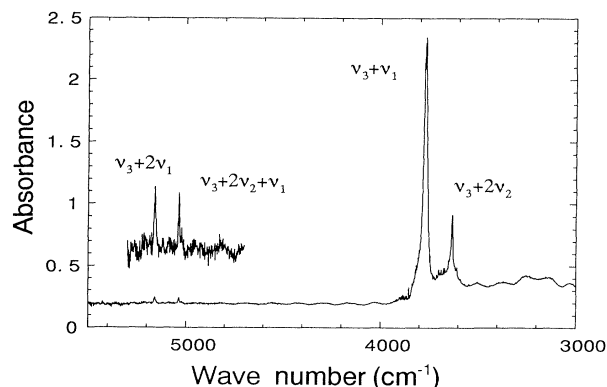


FIG. 1. Infrared absorption spectrum of cubic CO<sub>2</sub> measured at 8.9 GPa and room temperature. Approximate locations are 3632 ( $\nu_3+2\nu_2$ ), 3771 ( $\nu_3+\nu_1$ ), 5037 ( $\nu_3+2\nu_2+\nu_1$ ), and 5160 cm<sup>-1</sup> ( $\nu_3+2\nu_1$ ).

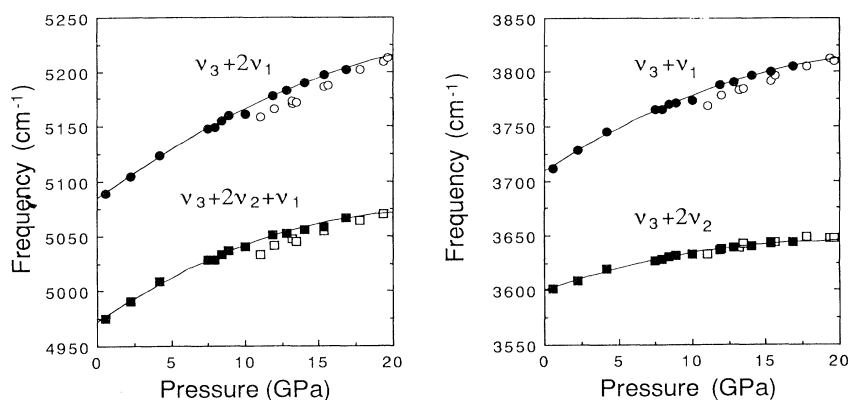


FIG. 2. Pressure dependence of the  $\nu_3+2\nu_2$ ,  $\nu_3+\nu_1$ ,  $\nu_3+2\nu_2+\nu_1$ , and  $\nu_3+2\nu_1$  combination bands. The solid and open symbols represent the frequencies for the *Pa3* and high-pressure phases, respectively. The solid lines are least-square fits to the data for the *Pa3* phase.

$\nu_3$  modes are infrared active. Absorption associated with the normal vibrations was too strong; their band positions were unable to be determined due to saturation. For the combination bands of  $\nu_3+2\nu_2$ ,  $\nu_3+\nu_1$ ,  $\nu_3+2\nu_2+\nu_1$ , and  $\nu_3+2\nu_1$  with adequate absorption intensity, the vibrational frequencies were observed over the whole pressure range measured.

Figure 1 shows a typical ir spectrum of the cubic phase measured at 8.9 GPa. Although the absorption bands broadened somewhat owing to an increase in the pressure gradient and a strengthening of intermolecular interactions, their full bandwidths were still around  $10\text{ cm}^{-1}$ , sufficiently sharp for accurate determination of the positions. The strongest peak around  $3771\text{ cm}^{-1}$  is the  $\nu_3+\nu_1$  combination band. The  $\nu_3+2\nu_2$  peak with medium intensity is located at  $3632\text{ cm}^{-1}$ . Two weak peaks at  $5037$  and  $5160\text{ cm}^{-1}$  are  $\nu_3+2\nu_2+\nu_1$  and  $\nu_3+2\nu_1$  combination bands, respectively.

The pressure dependences of the combination bands are shown in Fig. 2, in which the frequencies measured on loading and unloading processes are plotted together. Although the high-pressure phase appeared above 12 GPa in the first compression, a large hysteresis of the transition pressure in the second compression allowed the spectra of the low-pressure phase to be collected for a wide pressure range beyond the transition pressure. The observed frequencies ( $\text{cm}^{-1}$ ) of the cubic and high-pressure phases were fit to second-order polynomials in pressure  $P$  (GPa). The results are summarized in Table I along with the previous results for the gas<sup>10</sup> and cubic

phases.<sup>11</sup> The frequencies of  $\nu_3+2\nu_1$ ,  $\nu_3+\nu_1$ , and  $\nu_3+2\nu_2+\nu_1$  of the high-pressure phase are located about  $10\text{--}20\text{ cm}^{-1}$  below those of the cubic phase, while the frequency change in  $\nu_3+2\nu_2$  is small.

Transition pressure was significantly affected by pressure history of the specimen as shown in Fig. 3. The transition from the cubic phase occurred abruptly at 12 GPa in the first compression, accompanying a jump in the frequency by about  $10\text{ cm}^{-1}$ . From Raman spectra (see the upper spectrum in Fig. 4), the high-pressure phase was identified with that reported by Hansen,<sup>4</sup> although the transition pressure was about 6 GPa lower and only two libron peaks, instead of three peaks as previously reported, were observed. The libron peaks from the low-pressure cubic phase completely disappeared.

While the pressure was released from 17.8 GPa, the highest pressure reached in the first run, a reverse transformation to the cubic phase occurred below 10 GPa. The phase boundary initially situated between two ruby chips separated by approximately  $100\text{ }\mu\text{m}$ , whose fluorescence peaks indicated pressures of 9 and 10 GPa, moved slowly to the higher pressure side and after a few hours the low-pressure cubic phase filled the gasket hole. The pressure and its gradient remained unchanged during the microscope observation. In the second compression, the transition proceeded very sluggishly above 16 GPa. The presence of the cubic phase was confirmed in the spectrum even at 19.6 GPa as seen in the lower spectrum of Fig. 4. The hysteresis thus obtained was about 6 GPa.

TABLE I. Infrared vibrational modes of solid  $\text{CO}_2$ . The ir frequencies of the cubic phase in the range 0.6–16 GPa and those of the high-pressure phase in the range 11–20 GPa are expressed as a polynomial of form  $A+BP+CP^2$ .

Mode	Previous work			Present work						
	Gas phase <sup>a</sup>	Cubic phase <sup>b</sup>			Cubic phase			High-pressure phase		
		A	B	C	A	B	C	A <sup>c</sup>	B	C
$\nu_3+2\nu_2$	3612.8	3598.3	57	-23	3600.3	45	-12	3633.4	84	-22
$\nu_3+\nu_1$	3714.8	3707.6	99	-33	3708.6	87	-17	3770.8	99	-17
$\nu_3+2\nu_2+\nu_1$	4977.8	4970	104	-37	4971.6	89	-20	5034.4	80	-12
$\nu_3+2\nu_1$	5099.6	5084.8	107	-35	5083.9	97	-16	5158.6	62	0

<sup>a</sup>Reference 10.

<sup>b</sup>Reference 11.

<sup>c</sup>Frequencies at 11 GPa.

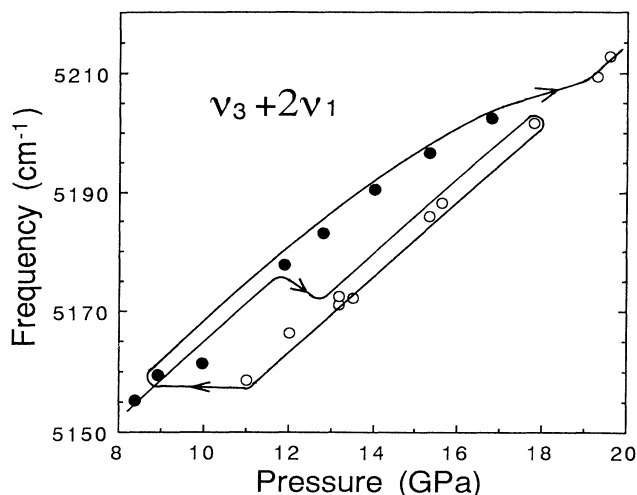


FIG. 3. The  $\nu_3 + 2\nu_1$  combination frequency measured by cyclic loading and unloading experiments. The solid and open circles represent the frequencies for the  $Pa3$  and high-pressure phases, respectively. The trajectory indicates the pressure history.

#### DISCUSSION

The vibron frequencies in solid CO<sub>2</sub> were measured over a wide pressure range for both the low- and high-pressure phases. These vibrational data reflect the molecular arrangement or the intermolecular interactions in the high-pressure phase and therefore allows consideration into the possible crystal structure. The theoretically

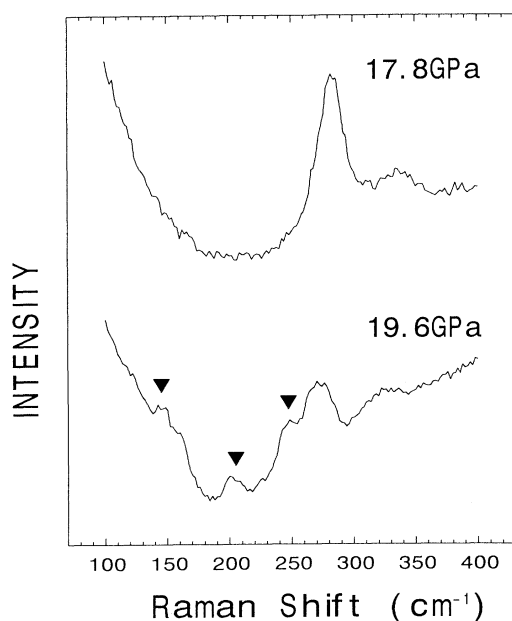


FIG. 4. Raman spectra of solid CO<sub>2</sub> measured at 17.8 GPa in the first compression (the upper spectrum) and at 19.6 GPa in the second compression (the lower spectrum). Solid triangles indicate the Raman peaks from the cubic phase.

predicted  $Cmca$  structure will first be tested by comparing the experimental results with the calculation and then a tetragonal  $P4_2/mnm$  structure, another candidate structure for densified solid CO<sub>2</sub>, will be examined.

The frequency shifts of the normal modes,  $\nu_i(P) - \nu_i(0)$ , were calculated from the observed combination frequencies. They are plotted in Fig. 5 along with those obtained by the theoretical calculations.<sup>9</sup> In the cubic phase, the calculated results agree well with the experimental data, reproducing the overall aspects of the frequency shifts measured for the stretching  $\nu_1$  and  $\nu_3$  modes and the bending  $\nu_2$  mode. These good agreements indicate that the potential model correctly describes the interactions between CO<sub>2</sub> molecules over a wide pressure range and is therefore justified in its application to the high-pressure phase.

The agreement is rather poor in the high-pressure phase. The frequency changes associated with the transition, for instance, were not correctly obtained. The calculation predicted a frequency decrease for all the normal modes and a remarkably large change in the antisymmetric stretching mode  $\nu_3$ . The actual measurement, however, revealed that the frequency of the bending mode  $\nu_2$  increased and the symmetric stretching mode  $\nu_1$  showed the largest decrease at the transition. By taking into account the agreement in the low-pressure phase, these discrepancies can be attributed to an incorrect model structure; the  $Cmca$  structure is inadequate for an explanation of the observed vibrational properties.

A tetragonal  $P4_2/mnm$  structure, isomorphic with a high-pressure  $\gamma$ -N<sub>2</sub>,<sup>12</sup> is another candidate for the high-pressure phase of solid CO<sub>2</sub>.<sup>8,9</sup> The molecules are arranged in parallel within a layer with the molecular axes inclining at 45° in respect to the crystalline  $a$  axes. This peculiar molecular arrangement (it is worthwhile to recall here that in the  $Cmca$  structure the molecules are ar-

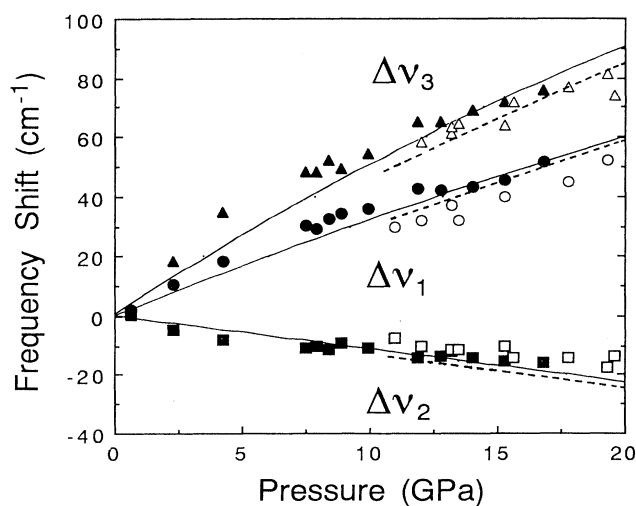


FIG. 5. Pressure dependence of the  $\nu_1$ ,  $\nu_2$ , and  $\nu_3$  normal-mode frequencies. The solid symbols and lines represent the vibron frequencies for the  $Pa3$  phase measured and calculated,<sup>9</sup> respectively. The open symbols and dashed lines give the same information for the high-pressure phase.

ranged perpendicular to each other in layers) probably brings relaxation in the potentials for the stretching vibrations and tightening in those for the bending motions. With this potential model, although it may be too oversimplified, the large decrease in  $\nu_1$  and the increase in  $\nu_2$  at the transition are qualitatively explained.

The libron spectrum is another experimental result supporting the transition scheme from the  $Pa3$  to  $P4_2/mnm$  structure. The tetragonal unit cell contains two molecules and hence only two librational modes are expected in the first-order Raman spectrum. This is consistent with the present Raman results; only two libron peaks were observed as in the high-pressure  $\gamma$  phase of solid  $N_2$  with the same  $P4_2/mnm$  structure.<sup>13</sup>

The main argument, which has been ruling out the tetragonal structure as the high-pressure phase, arises from discrepancy in the number of Raman active mode. In the previous measurements<sup>4,5</sup> three or four libron peaks were observed for the high-pressure phase. This is apparently inconsistent with the predicted libron spectrum of the tetragonal structure. However, as is also shown in their measurements, the weak peaks disappeared on further compression and two peaks were distinctly observed at a higher-pressure region above 18 GPa. This may be explained by the gradual transformation of the residual cubic phase with increasing pressure. The librational peaks from the cubic phase were additionally observed for a while after the transition; the high-pressure phase essentially possesses two libron peaks. Thus, both the vibron and libron spectra lead to a conclusion that the tetragonal  $P4_2/mnm$  structure is the more likely structure as the high-pressure phase of solid  $CO_2$ .

A large hysteresis is one remarkable feature of the phase transition in solid  $CO_2$ . The low- and high-pressure phases exist together over a very wide pressure range from 10 to 20 GPa. This implies the presence of a large potential barrier between the two structures. Etters and Kuchta<sup>9</sup> showed in their calculation that the potential barrier for the transition from the cubic to the  $Cmca$  structure is about 235 K and is increased to 1100 K much

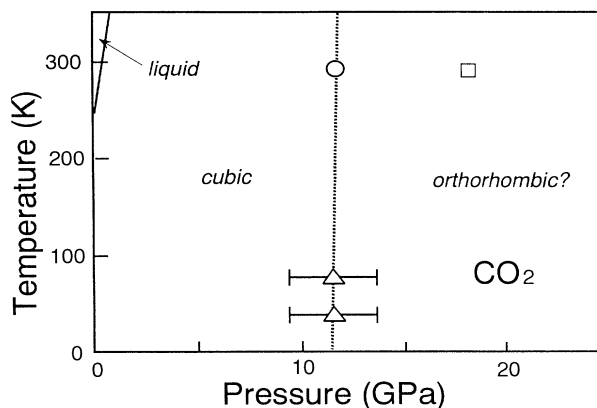


FIG. 6. Tentative phase diagram of  $CO_2$ . Solid line represents the boundary between the liquid and cubic phases. ○: Present work. □: Reference 4. △: Reference 5.

higher for the transition to the tetragonal structure. In either structure the potential barrier associated with rotations of  $CO_2$  molecules results in large hysteresis in the transition. The potential barrier to be overcome gets higher by the presence of dislocations or particle boundaries which are introduced in the specimen through the phase transition. Consequently, the second transition is inhibited and its transition pressure is pushed away from the first transition pressure of 12 GPa.

Finally a tentative phase diagram of  $CO_2$  is presented in Fig. 6. The transition in the cubic phase occurs from 12 to 16 GPa at room temperature depending on pressure history of the specimen. The lower pressure of 12 GPa is very close to the transition pressures at low temperatures of 40 and 80 K, indicating that the transition is temperature insensitive. There has been another room-temperature transition reported above 6 GPa.<sup>5</sup> No signal indicating the phase change was detected in the present ir measurement. This is consistent with the results of the previous Raman<sup>4</sup> and the recent Brillouin<sup>14</sup> measurements.

<sup>1</sup>W. H. Keesom and J. W. L. Kohler, *Physica* **1**, 167 (1934).

<sup>2</sup>B. Olinger, *J. Chem. Phys.* **77**, 6255 (1982).

<sup>3</sup>L. Liu, *Earth Planet. Sci. Lett.* **71**, 104 (1984).

<sup>4</sup>R. C. Hanson, *J. Phys. Chem.* **89**, 4499 (1985).

<sup>5</sup>H. Olijnyk, H. Dafer, H.-J. Jodl, and H. D. Hochheimer, *J. Chem. Phys.* **88**, 4204 (1988).

<sup>6</sup>K. Kobashi and T. Kihara, *J. Chem. Phys.* **72**, 3216 (1980).

<sup>7</sup>R. LeSar and R. G. Gordon, *J. Chem. Phys.* **78**, 4991 (1983).

<sup>8</sup>B. Kuchta and R. D. Etters, *Phys. Rev. B* **38**, 6265 (1988).

<sup>9</sup>R. D. Etters and B. Kuchta, *J. Chem. Phys.* **90**, 4537 (1989).

<sup>10</sup>I. Suzuki, *J. Mol. Spectrosc.* **25**, 479 (1968).

<sup>11</sup>R. C. Hanson and L. H. Jones, *J. Chem. Phys.* **75**, 1102 (1981).

<sup>12</sup>R. L. Mills and A. F. Schuch, *Phys. Rev. Lett.* **23**, 1154 (1969).

<sup>13</sup>F. D. Medina and W. B. Daniels, *J. Chem. Phys.* **64**, 150 (1976).

<sup>14</sup>H. Shimizu, T. Kitagawa, and S. Sasaki, *Phys. Rev. B* **47**, 11 567 (1993).